0022-202X/83/8106-0489$02.00/0
THE JOURNAL OF INVESTIGATIVE DERMATOLOGY, 81:489–497, 1983

Vol. 81, No. 6
Printed in U.S.A.

Ultrastructure and Three-Dimensional Reconstruction of Several Macular and Papular Telangiectases

IRWIN M. BRAVERMAN, M.D. AND AGNES KEH-YEN, M.S., B.S.

Department of Dermatology, Yale University School of Medicine, New Haven, Connecticut, U.S.A.

Eight types of telangiectases were studied by light and electron microscopy and by 3-dimensional reconstruction from photomicrographs. Five were macular: mat telangiectasia of scleroderma, generalized essential telangiectasia, nevus flammeus, and 2 macular types not previously described. Three were papular: cherry angioma, angiokeratoma (Fabry), and angiokeratoma (Fordyce).

The macular telangiectases were produced by dilatation of postcapillary venules of the upper horizontal plexus. There was no evidence of neovascularization or vascular malformation. The walls of the dilated venules were thickened by the peripheral deposition of basement membrane-like material admixed with reticulin fibers.

The ultrastructure and configuration of the papular telangiectases were different. The cherry angioma was produced by spherical and tubular dilatations of capillary loops in dermal papillae. Each abnormally dilated loop was connected to the neighboring loop or loops by tortuous vascular channels. The vessels in the upper horizontal plexus were not involved. Ultrastructurally, the cherry angiomas were composed of both venous capillaries and postcapillary venules whose walls were thickened in a manner identical to that observed in the macular telangiectases. The angiokeratomas of Fabry and Fordyce were also produced by vascular abnormalities predominantly involving the dermal papillae. Ultrastructurally these vessels were similar to the small collecting veins which are normally found at the dermal–subcutaneous interface. Thus, the papular telangiectases also arose by alterations of the existing microvasculature rather than by proliferation of new vessels with random anastomoses.

Reconstruction of the upper horizontal plexus from normal skin showed an undulating network of arterioles and their accompanying postcapillary venules. A 3-layered plexus arranged as venules, arterioles, and venules was not found.

Telangiectases have diverse forms. Although some are diagnostic markers for systemic disease (e.g., the mat telangiectasia of scleroderma, the angiokeratoma of Fabry's disease, and the red puncta of hereditary hemorrhagic telangiectasia), most telangiectases are considered to be cosmetic problems without any medical significance. The telangiectases have not been studied extensively either by ultrastructure or in 3 dimensions. As a first step toward understanding their etiology, it is necessary to determine the ultrastructure and 3-dimensional configuration of these microvascular abnormalities. Are they formed by the dilatation of existing vessels or by the proliferation of new vessels? If proliferation has occurred, do the vascular formations represent random anastamoses or well-organized 3-dimensional networks? In this paper we describe the ultrastructure and 3-dimensional configurations of 8 types of telangiectases which can be divided into 2 mutually exclusive groups: those that represent abnormalities of the upper horizontal plexus without involvement of the capillary loops in the dermal papillae and those that are characterized by vascular abnormalities in the dermal papillae without involvement of the horizontal plexus.

Manuscript received January 4, 1982; accepted for publication July 20, 1983.

Reprint requests to: Irwin M. Braverman, M.D., Department of Dermatology, Yale University School of Medicine, 333 Cedar Street, New Haven, Connecticut 06510.

MATERIALS AND METHODS

Telangiectases were removed partially or entirely by 3- or 4-mm punches from areas of skin which had been anesthesized in a circle with 1% lidocaine without epinephrine. In this fashion, the lesions were not traumatized by the anesthesia. Small portions of the lesions were prepared for electron microscopy by techniques described previously [1]. The major portions were similarly processed and embedded in Spurr's resin for use in the subsequent reconstructions. Three-dimensional models were constructed from photomicrographs of serial 1-μm sections. Every second or fourth section was photographed; string was glued to the profiles of the vessels to outline them; the extravascular and intravascular portions of the photograph were cut away; and one layer was glued to the next. The first photograph in the series was left intact so that the epidermis and dermis could serve as a background of orientation for the 3-dimensional model. The dimensions of the reconstructed lesions ranged from 220–1800 μm in any 1 of their 3 axes. The precise measurements for each reconstruction are given later in the text. The smaller portions of each lesion were examined by electron microscopy for determination of the ultrastructure in various parts of the model.

In 4 of the 5 models constructed, the Z axis (the extension of the model parallel to the epidermal surface) was not in proportion to the height (Y axis) and width (X axis) of the sections from which the model was made (see Fig 1). The Z axis was corrected by determining the total magnification of the photographs of the sections from which the models were made and then calculating, by direct measurements on the completed model, how much the Z axis had been enlarged. The Z axis was 1.8–2.6 times greater than it should have been. To correct for this discrepancy the following steps were taken. A 2-dimensional drawing of the model in its actual dimensions was made; multiple, evenly spaced horizontal lines were drawn perpendicular to the Z axis; and the distance between each pair of lines was reduced by the amount necessary to bring the Z axis into proportion with the Y and X axes of the tissue section. A drawing of the model was then made to the correct scale with the Z axis having been reduced by the appropriate amount. In some instances, we have included schematic drawings along with the actual models and their renderings so that the complex vascular relationships within these telangiectases may be better understood. A clay reconstruction was made of one telangiectatic lesion because it was too complex to be rendered in a drawing. As controls for these studies we reconstructed the upper horizontal vascular plexus from the flexor forearm skin of a healthy 22-year-old woman. During the past decade we have also studied the upper horizontal plexus in 1-μm and ultrathin sections in over 100 patients ranging in age from 6–90 years. These specimens have been obtained from all parts of the skin surface including the face and have been obtained from normal healthy volunteers as well as from patients with diabetes, psoriasis, eczema, and vasculitis. We have never observed abnormalities in the upper horizontal plexus by these techniques that would suggest that the basic organization of the upper horizontal plexus is altered by age or body site in normal individuals or in patients with the disorders listed above.

This paper reports our studies on the following varieties of telangiectases. Two of them have not been described previously to our knowledge and are indicated by an asterisk. The other varieties are firmly established clinical entities. *Type I*—idiopathic macular telan-*

giectasia. Bright red patches consisting of fine wiry vessels were present over the extensor surfaces of the limbs, on the malar areas of the chin, on the superior chest and midabdomen adjacent to the umbilicus, over the buttocks, and over the toes in 2 men aged 17 and 60 years. Some of the patches were slightly reticular and others were extensive and uniform. There were also a few 2- to 5-cm patches scattered over the rest of the body. No underlying disease was detected and the lesions had been present for several years before the patients were studied. Biopsies were taken from the extensor surface of the thigh in one patient and from the extensor surface of the forearm in the other. *Type II—generalized essential telangiectasia as described by McGrae and Winkelmann [2].* This disorder seen primarily in women first appears about age 30–40 years. The eruption appears first on the feet and legs and spreads to involve the thighs, trunk and arms. Three types of lesions are present: venous stars (superficial varicosities) on the feet and legs, diffuse areas of bright erythema produced by fine wiry vessels on the extensor surfaces of the legs, 4- to 10-mm and telangiectatic macules in which one can see the fine wiry vessels. No underlying disease is present. Three women aged 40, 50, and 54 were studied. Biopsies were taken of the macules and of the areas of diffuse erythema on the abdomen and upper thighs, respectively. *Type III—telangiectatic mats of scleroderma.* These lesions are red to pink macules, 2–30 mm in diameter or width, in which individual vessels cannot be seen clinically. The mats are present only on the face, lips, tongue, palate, superior chest, and hands. Two men aged 35 and 65 and 1 woman aged 85 were studied. Biopsies were taken of mats from the medial aspect of the arm adjacent to the axilla, from the palm of the hand, and from the chest and tongue of a person at autopsy. *Type IV*—telangiectatic mats identical in appearance to those of scleroderma.* Two women aged 59 and 70 were studied. Both had psoriasis but no other underlying disease. In one patient the mats were generalized over the entire body, and in the other, there were only a few mats which were localized to the chest and abdomen. In both women, biopsies of the mats on the abdomen were obtained. *Type V—nevus flammeus.* Biopsy was performed on a nevus flammeus at the angle of the jaw in a 60-year-old man. *Type VI—cherry angioma (Campbell de Morgan spot).* Three lesions in 2 women, 30 and 50 years old, were studied. The angiomas were obtained from the superior back and midabdomen. They measured 0.2 mm, 0.5 mm, and 1.0 mm in diameter. Models were built from portions of the 0.2-mm and 1.0-mm lesions. *Type VII—angiokeratoma of Fabry (angiokeratoma corporis diffusum).* An angiokeratoma, 1.0 mm in diameter, which was present on the anterior thigh of a 40-year-old man with Fabry's disease was biopsied for study. *Type VIII—angiokeratoma of the scrotum (Fordyce).* An angiokeratoma, 2.5 mm in diameter was removed from the scrotum of a 70-year-old man. In these last 3 telangiectases we included margins of normal skin on both sides of the telangiectases in the reconstructions.

These studies were approved by the Human Investigation Committee at Yale.

RESULTS

Controls

Figs 1 and 2 show the 3-dimensional reconstruction of the upper horizontal plexus in a model and in a detailed drawing, respectively. The black arrowheads in each figure point to the same vessel. The upper horizontal plexus occupied the papillary dermis and the most superficial portion of the reticular dermis. The volume of dermis represented by the model, exclusive of the epidermal layer, measured 1400 μm wide (X axis), 120 μm high (Y axis), and 260 μm deep (Z axis). The postcapillary venules and the arterioles with their accompanying venules pursued an undulating course through the entire region occupied by the horizontal plexus. Some vessels from the upper papillary dermis coursed toward the lower levels and some undulated between the upper and mid levels. Arterioles and their accompanying venules frequently bifurcated to join adjacent arterioles and venules to produce a vascular net. We found no vascular configurations to indicate that the horizontal plexus was composed of a 3-tiered system (venule–arteriole–venule) with shunts connecting the first and third layers. The majority of vessels in the normal upper horizontal plexus were postcapillary venules.

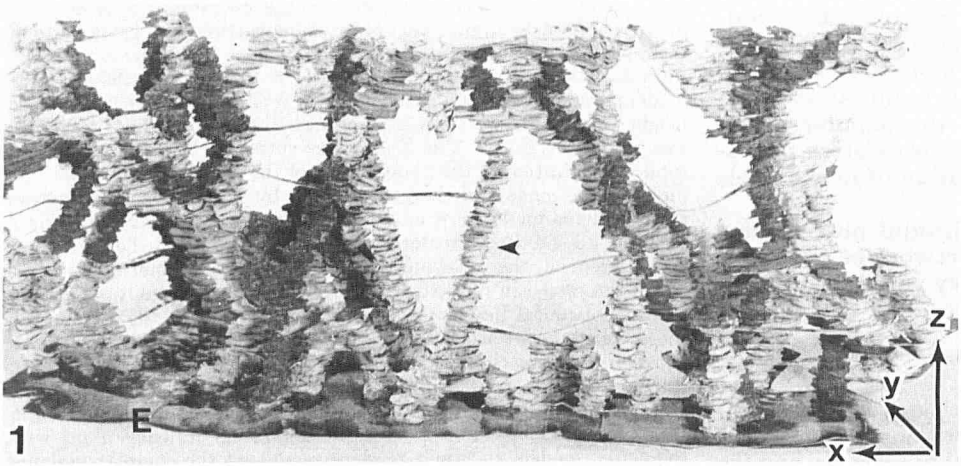

FIG 1. Model of horizontal plexus from forearm skin. *White vessels* = postcapillary venules. *Dark vessels* = arterioles. *Arrowhead* points to identical vessels in Figs 1 and 2. *E* = location of epidermis on first photograph in the series used for construction of model. The plexus is being viewed in its horizontal (Z) plane from the epidermal surface. The *X*, *Y*, and *Z* axes of the model are shown in the right corner.

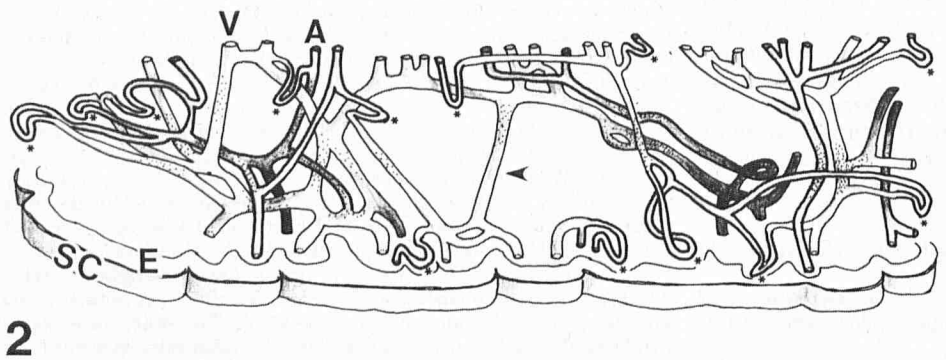

FIG 2. Detailed drawing of the model in Fig 1. *SC* = stratum corneum surface. *E* = epidermis. Narrow vessels with bold outlines (*A*) = arterioles. Wide vessels with thin outlines (*V*) = postcapillary venules. *Nonshaded portions* of both vessels are in superficial layer of papillary dermis; *stippled areas* are in the midpapillary dermis; and *completely shaded areas* are in deep papillary dermis. *Asterisks* indicate hairpin capillary loops in dermal papillae. Shading of vessels indicates undulating course of plexus.

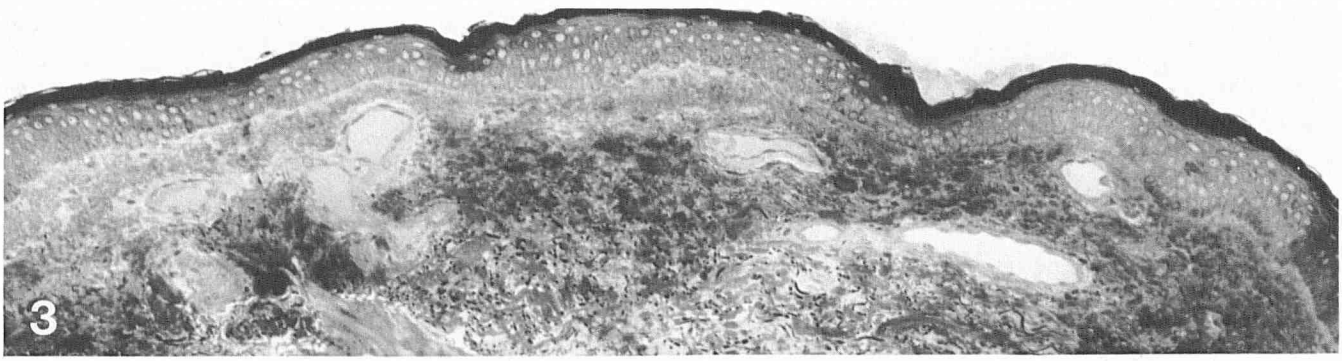

FIG 3. Histology of telangiectatic mat of patient with scleroderma. The vessels in the papillary dermis are abnormally dilated. All the telangiectases of types I–V showed this pattern. One-μm section, Spurr's resin, × 174.

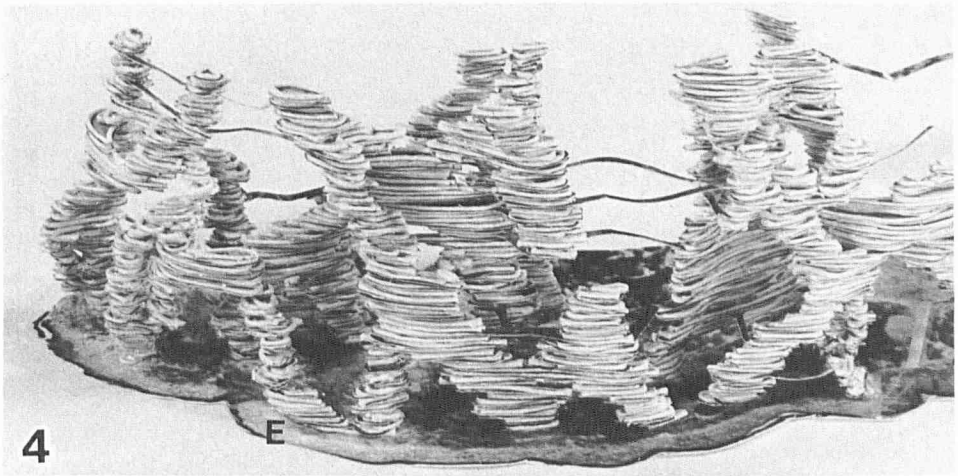

FIG 4. Model of telangiectatic mat of scleroderma. Orientation, size, and scale of model identical to that of Fig 1. Venular dilatation is 3–5 times normal, but the venular pattern is similar to that of the normal upper horizontal plexus.

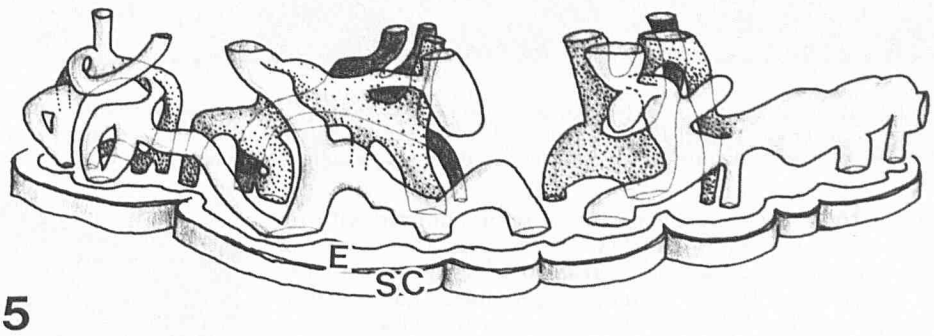

FIG 5. Drawing of telangiectatic mat shown in Fig 4 *SC* = stratum corneum surface. *E* = epidermis. The dilated venules are being viewed in their horizontal (Z) plane from the epidermal surface. *Nonshaded vessels* are in superficial layer of papillary dermis, *stippled vessels* are in midpapillary dermis, and *completely shaded areas* are in deep papillary dermis. Drawing has been made to the same scale as Fig 2.

Macular Telangiectases (Types I–V)

All of the telangiectases (types I–V) were similar by light and electron microscopy. Representative histology of these lesions is shown in Fig 3. Although we reconstructed only the telangiectatic mat of scleroderma, examination of the serial 1-μm sections from the other 4 types showed patterns of vascular dilatation similar to those seen in the lesion of scleroderma. The model and detailed drawing of the telangiectatic mat of scleroderma are shown in Figs 4 and 5 and are the prototype for types I–V. The model represents a volume of tissue 1800 μm wide (X axis), 120 μm high (Y axis), and 288 μm deep (Z axis). The drawing shows that some dilated vessels pass from the upper toward the lower portions of the papillary dermis just as the vessels in the normal papillary dermis do. The dilated vessels formed a vascular network as they branched and joined one another in the horizontal plane and as they undulated and joined their neighbors in the vertical plane of the papillary dermis.

Electron microscopy showed that the vascular dilatations were confined to postcapillary venules as identified by multilaminated basement membrane in the vascular wall (Fig 6, arrow), incomplete to complete investment by pericytes, absence of bridged fenestrations in the endothelial cells, and the presence of individual collagen fibrils throughout the wall. Veil cells were also present. Arterioles were not found in any of these telangiectatic lesions. The venules in these 5 types of telangiectasia were dilated 3–5 times normal. Except for this marked dilation, the venular pattern was identical to that of the normal horizontal plexus.

The walls of the dilated postcapillary venules were thickened to 6–10 μm (normal 3–5 μm) by the addition of morphologically

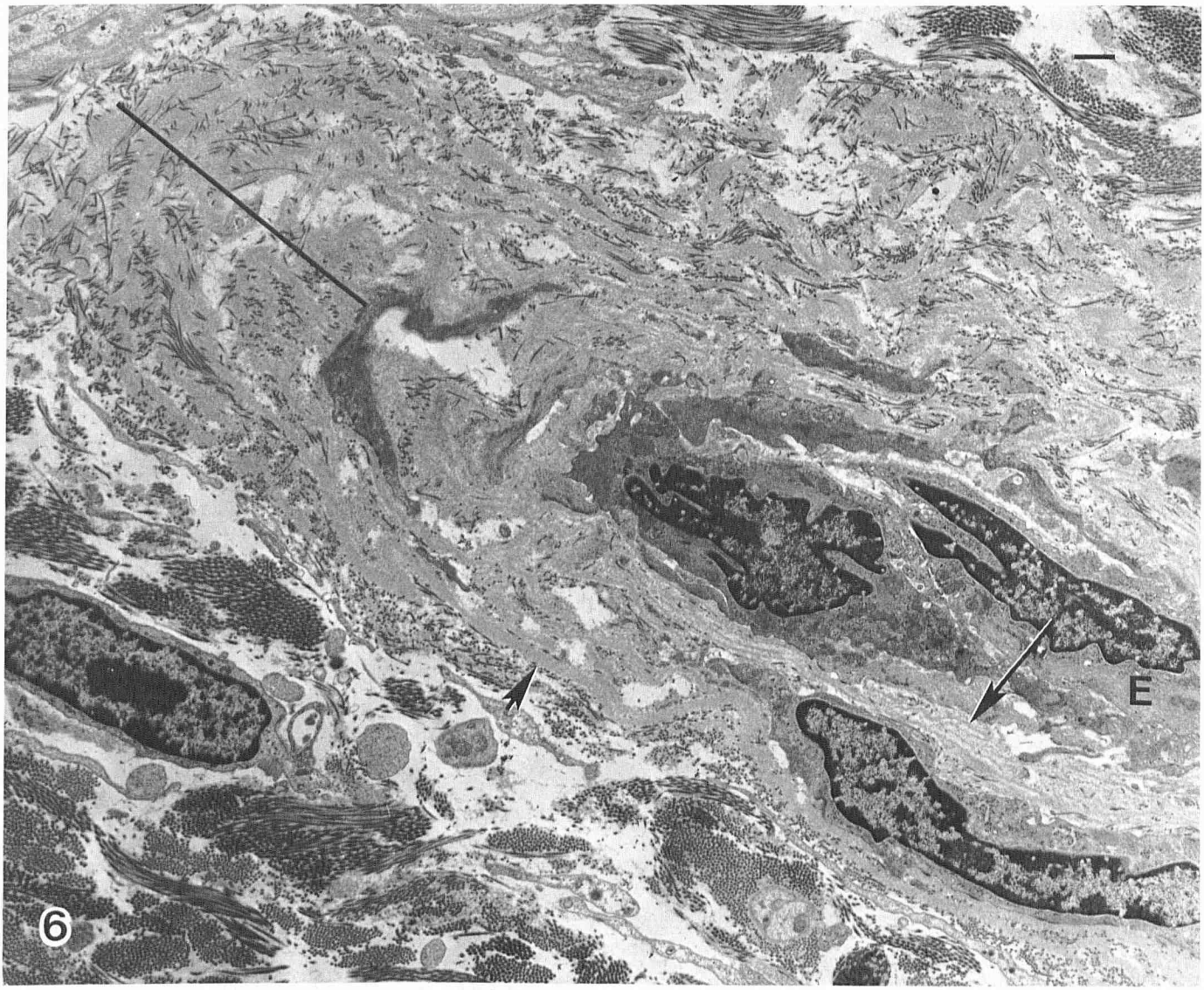

FIG 6. Postcapillary venule in telangiectatic mat of scleroderma. *E* = endothelial cell with collapsed lumen. *Arrow* indictes normal multilayered basement membrane material in vascular wall. *Arrowhead* and *black line* indicate belts of basement membrane-like material admixed with reticulin (collagen fibrils) that have been deposited around vascular wall. *Bar* = 1 μm.

homogeneous basement membrane material admixed with reticulin fibers similar to the material seen in the vessels of actinically damaged skin and chronologically aging skin [3]. The cutaneous vessels of patients with diabetes mellitus (unpublished data) and the porphyrias [4] show the same changes. The deposition of this material was not related to any of these factors in our patients. The telangiectatic mat on the tongue of the patient with scleroderma was also composed of vessels having the ultrastructural characteristics of postcapillary venules with vascular wall thickening by an identical but narrower belt of basement membrane material admixed with reticulin fibers. Veil cells were also present in the specimen from the tongue but in fewer numbers than normally seen around comparable vessels in the skin.

Papular Telangiectases (Types VI–VIII)

Type VI—cherry angioma: Fig 7 is a 1-μm section from the 1.0-mm cherry angioma. The outlined area indicates the site from which the model in Fig 8 was built. Normal skin is present to the extreme left of the outlined area and to the right as well (not shown). In almost all of the 1-μm sections there was a single profile of markedly dilated vessel in each papilla with 1

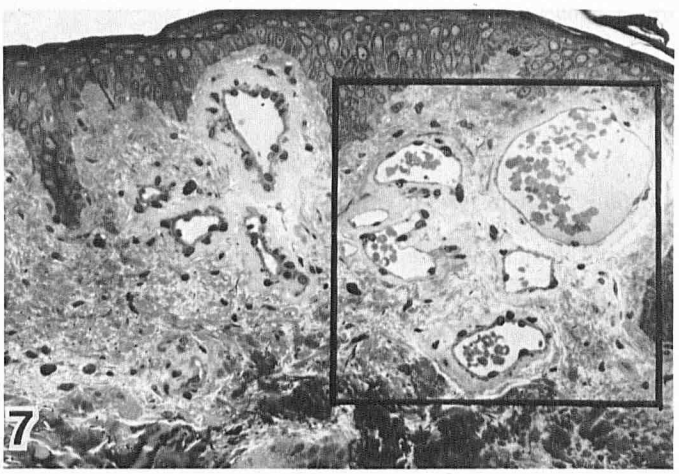

FIG 7. Histology of cherry angioma. The *outlined area* indicates the site from which the model in Fig 8 was constructed. Each papilla contains a single dilated vascular profile with smaller vascular profiles below them in papillary dermis. Vascular walls are thickened. One-μm section, Spurr's resin, × 370.

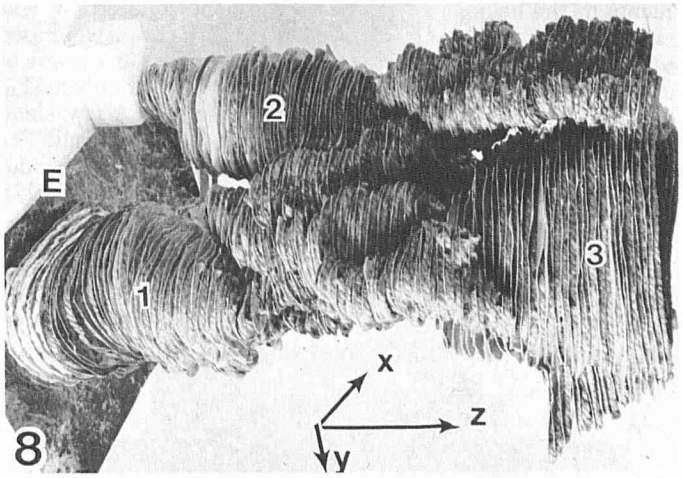

FIG 8. Photograph of model of cherry angioma. *E* = location of epidermis on the first photograph in the series used for construction of model. *X*, *Y*, and *Z* axes indicated in lower center. Epidermis is on X axis and dermis is on Y axis. Dilated portions of vessels in individual papillae are *numbered* and correspond to those in Fig 9. The intervening areas on the model are composed of the tortuous channels connecting the dilatations in each papilla.

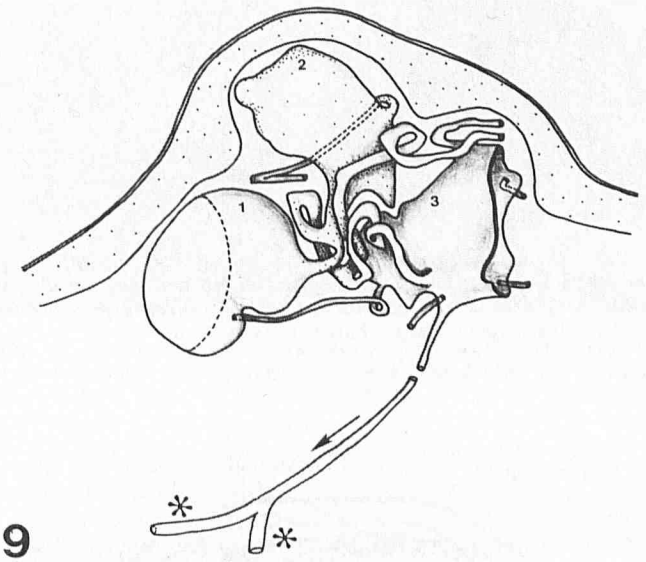

FIG 9. Cherry angioma. Drawing made in correct proportions. *Numbered dilated areas* correspond to those in Fig 8. *Arrow* indicates the connection between saccule *number 3* and postcapillary venule of horizontal plexus (*asterisks*). Connection is shown as an interrupted channel to keep angioma in proper scale.

or more smaller dilated vessels in the papillary dermis below the dermal papilla itself. In a few papillae, profiles of 2 or 3 dilated vessels, somewhat smaller in size, were seen. All of the dilated vessels had markedly thickened walls. The dimensions of the reconstructed angioma were 250 μm wide (X axis), 220 μm high (Y axis), and 228 μm deep (Z axis). Fig 9 shows a drawing of a portion of this angioma. There are 3 spherical vascular enlargements, each within its own papilla and connected to its neighbors by thin tortuous channels. The smaller vascular profiles observed below each papilla in Fig 7 represent these thin connecting channels. From the spherical dilatation labeled 3 (Fig 9), we were able to trace a direct connection to a normal postcapillary venule in the upper horizontal plexus (asterisks).

Although we did not include them in the model shown in Fig 8, further examination of many serial sections revealed a consistent pattern of vascular organization: one or more dilated vascular structures in each papilla was connected to its neighbor by vascular tubes of varying width (Fig 10).

In the reconstruction of the 0.2-mm cherry angioma we observed a papilla that contained a tubular dilatation which arose from the venous limb at the apex of capillary loop (Fig 11). The dilated portion occupied the entire papilla and displaced the loop from which it arose into the papillary dermis.

Electron microscopy revealed that the cherry angioma was composed of both dilated postcapillary venules and venous capillaries. In the postcapillary venules a belt of basement membrane-like material mixed with reticulin fibers was deposited around the normal multilaminated vascular wall (Fig 12). Zebra bodies or fibrous long-spacing fibers were numerous in these belts of basement membrane-like material and veil cells were prominent. The normal vascular wall of the postcapillary venules appeared to contain an increased amount of basement membrane material in areas because the normally laminated basement membrane (arrow) was not as distinctly laminated as it is normally. The abnormally thickened walls of the postcapillary venules ranged from 5–20 μm.

The endothelial cells of the venous capillaries had bridged fenestrations (Fig 13, arrowheads) and moderately thickened walls composed of loose basement membrane material mixed with reticulin fibers.

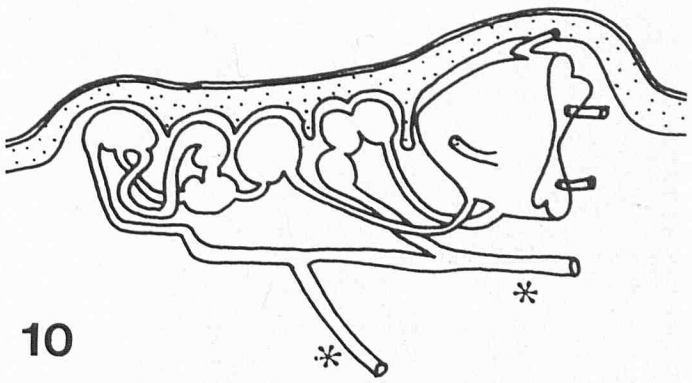

FIG 10. Cherry angioma. Schematic drawing based on serial sections immediately following saccule number 3 in Fig 9. One or more dilated vascular structures in each papilla is connected to its neighbor by channels of varying width. Connections to horizontal plexus (*asterisks*) are also shown.

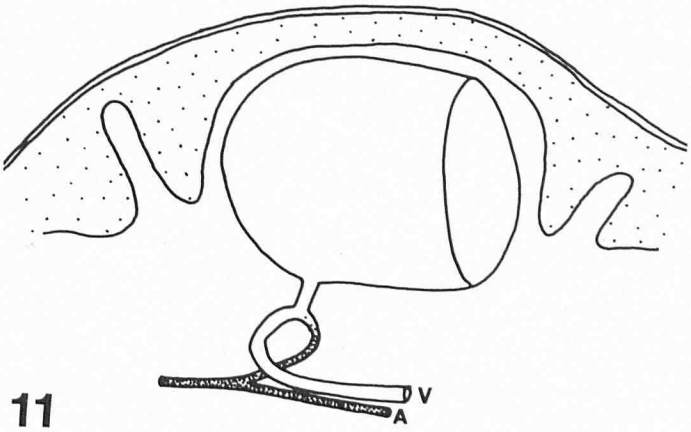

FIG 11. Cherry angioma. Reconstruction of a portion of 0.2-mm angioma showing dermal papilla filled with tubular dilatation arising from the venous limb at apex of capillary loop. The capillary loop has been displaced into the papillary dermis. *A* = arteriole and *V* = postcapillary venule of upper horizontal plexus.

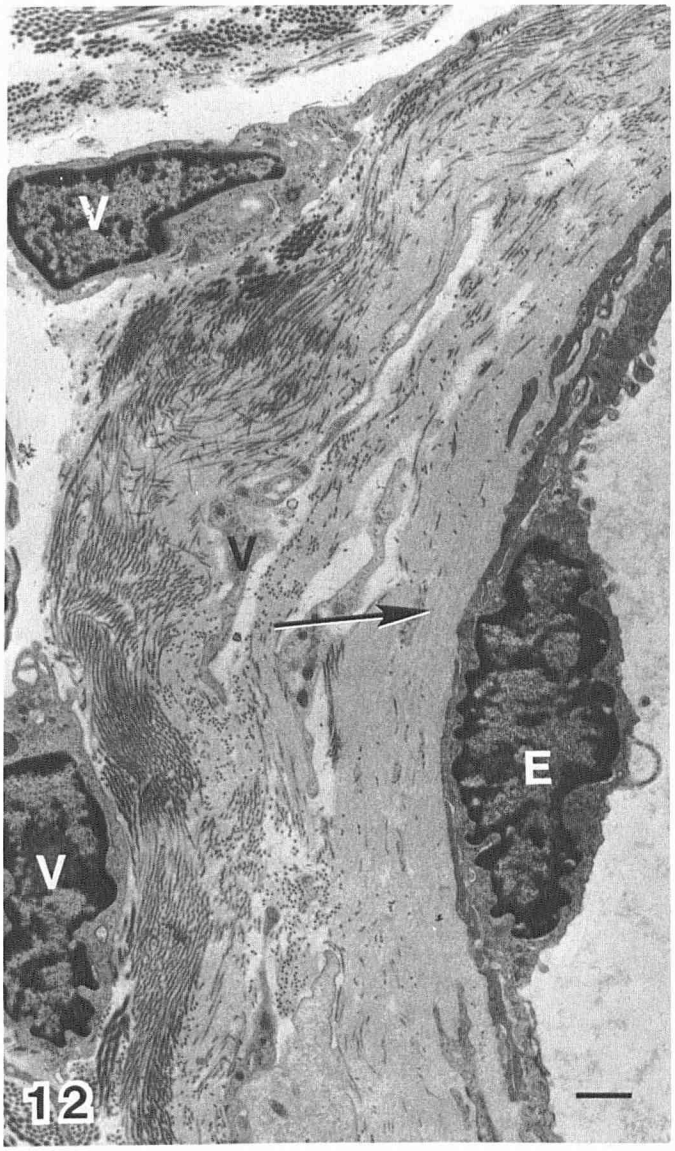

FIG 12. Wall of postcapillary venule. *Arrow* points to multilaminated basement membrane material in vascular wall that is not as distinctly laminated as it is normally. *V* = veil cells with adjacent belt of basement membrane-like material mixed with reticulin fibers which is responsible for the thickening of the vessel walls seen in Fig 7. *E* = endothelial cell. *Bar* = 1 μm.

Type VII—angiokeratoma (Fabry): The angiokeratoma was reconstructed almost in its entirety. It measured 950 μm wide (X axis), 1100 μm high (Y axis), and 424 μm deep (Z axis). A drawing of the model is shown in Fig 14. This telangiectasis consisted of a large tubular dilatation filling one papilla and 3 smaller serially connected dilatations filling an adjacent papilla. Both sets of saccules connected with 2 serially connected tubular dilatations immediately below in the papillary dermis. The entire complex made a final connection with a dilated vessel that passed directly into the deep dermis in a line perpendicular to the epidermal surface (Fig 15). This vessel most likely continued into the subcutaneous fat, but we have no direct evidence for this because the subcutaneous layer was not included in the biopsy block. This deep vessel contained 2 sets of valves (Figs 15, 16).

Electron microscopy showed that the portion of the angiokeratoma immediately beneath the epidermal surface consisted of endothelial cells lying on an irregularly thickened layer of focally multilaminated basement membrane material. The segments of the angiokeratoma adjacent to the collarette of epidermis (Fig 15, black arrowheads) had a vascular wall composed of homogeneous basement membrane material, 3 to 4 layers of smooth muscle cells, and many intervening collagen fibers (Fig 17). An internal elastic lamina was absent, but a few small fragments of elastic fibers were present in the vessel wall. The typical inclusions of Fabry's disease were present in the endothelial and smooth muscle cells and in the fibroblasts (Fig 17).

Type VIII—angiokeratoma of scrotum (Fordyce): This vascular lesion was larger than the cherry angioma and the Fabry lesion. A relatively smaller portion of the entire lesion was reconstructed compared to the other two papular telangiectases. The histology of the Fordyce lesion was composed of 2 compact clusters of dilated vessels each of which was contained within

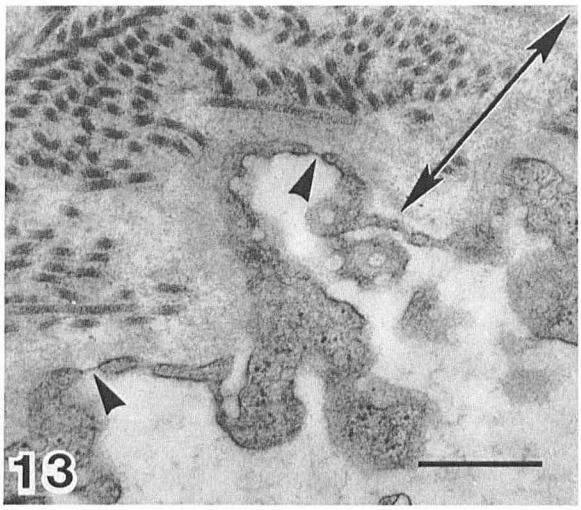

FIG 13. Cherry angioma. Venous capillary component with bridged fenestrations (*arrowheads*). Vascular wall thicker than normal and composed of loose-appearing basement membrane material mixed with reticulin fibers (*double-headed arrow*). *Bar* = 1 μm.

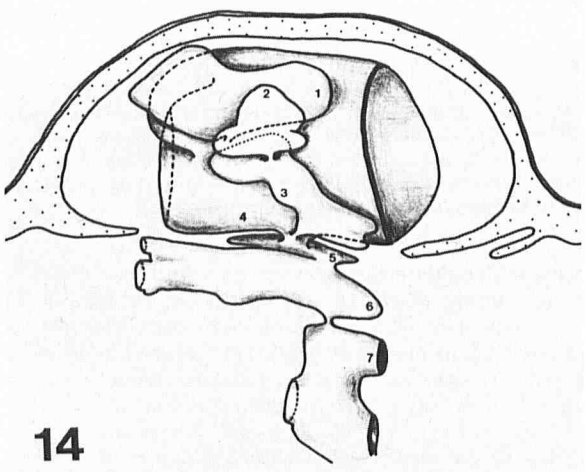

FIG 14. Drawing of model of Fabry lesion. The angiokeratoma occupied 2 papillae. Dilated saccule *4* was present in one and the serially connected saccules *1*, *2*, and *3* were in the other. Both sets connected with saccules *5* and *6* which in turn connected with a deep vessel labeled *7*. Additional sections beyond those shown in the drawing indicated that saccule *4* became a closed tube filling the entire dermal papilla.

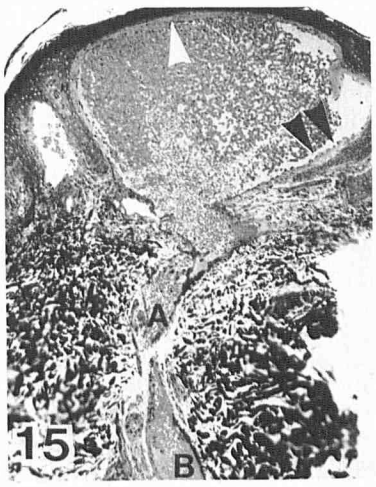

FIG 15. Histology of Fabry lesion shown in Fig 14. Dilated vascular portion in dermal papilla and papillary dermis connects with deep vessel which contains 2 sets of valves at *A* and *B*. *Arrowheads* indicate sites of examination by electron microscopy (see text for description). 1-μm section, Spurr's resin, × 145.

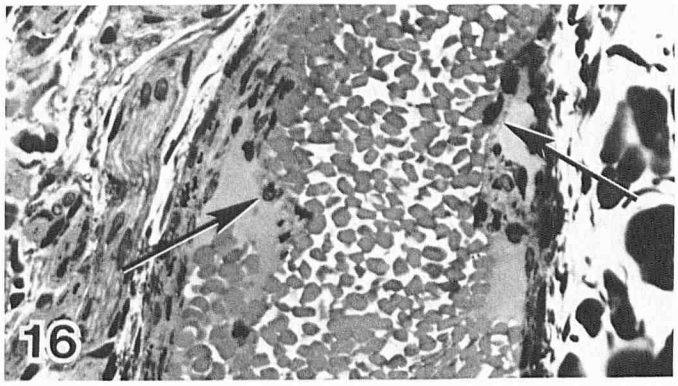

FIG 16. Histology of the connecting deep vessel shown in Fig 15. *Arrows* indicate 2 valve leaflets in vessel at site A. One-μm section, Spurr's resin, × 215.

a single, markedly widened dermal papilla. A portion of one of these widened papillae with its compact cluster is shown in Fig 18. The size of the reconstructed lesion measured 550 μm wide (X axis), 420 μm high (Y axis), and 536 μm deep (Z axis). The model and schematic drawing show that the reconstructed angiokeratoma consisted of spherical and tubular dilatations which were connected serially by very short, narrow channels (Figs 19, 20).

Although the Fordyce angiokeratoma was larger and therefore more complex in organization than the Fabry lesion, the segmental vascular dilatations showed the same short narrow connecting channels as seen in the Fabry lesion. However in the portion of the angiokeratoma examined, we did not find a vascular connection between the vessels of the Fordyce lesion in the papillary dermis and vessels in the deep dermis as we had in the Fabry lesion. Many serial sections beyond the drawing in Fig 20 showed that the papillary and reticular layers of the dermis above the dartos muscle were entirely occupied by dilated vascular segments that were serially connected. Since we did not reconstruct the entire lesion, we are unable to describe the location and nature of the deep dermal connection which must exist. However, by electron microscopy we found that the vessels of the Fordyce lesion were identical to those of the Fabry lesion. The ultrastructure of the dilated saccules just beneath the epidermis (Fig 18, arrowhead) was identical to that found in the Fabry lesion in the same location, and the fine structure of the dilated saccules in the deeper papillary dermis (Fig 18, 2 arrowheads) was identical to that shown in Fig 17 except for the absence of the abnormal cellular inclusions of Fabry's disease.

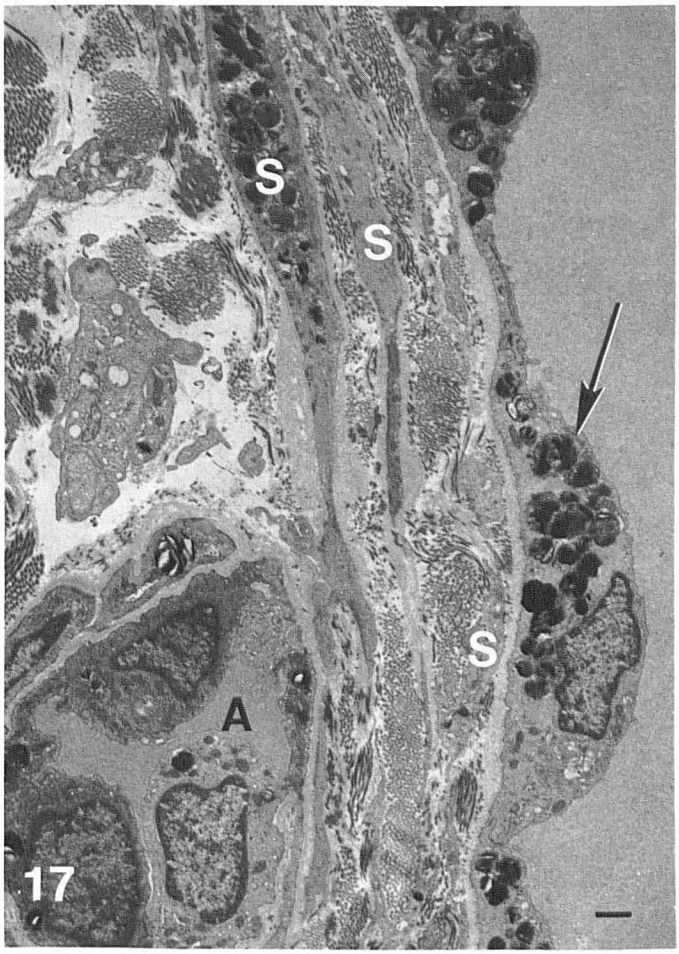

FIG 17. Angiokeratoma (Fabry). Ultrastructure at site indicated by the 2 black arrowheads in Fig 15. Note layers of smooth muscle cells (*S*) with intervening bundles of collagen fibers. Basement membrane material is homogeneous in appearance. An internal elastic lamina is not present. *Arrow* indicates cellular inclusions of Fabry's disease in endothelial cell. *A* = normal sized adjacent arteriole. *Bar* = 1 μm.

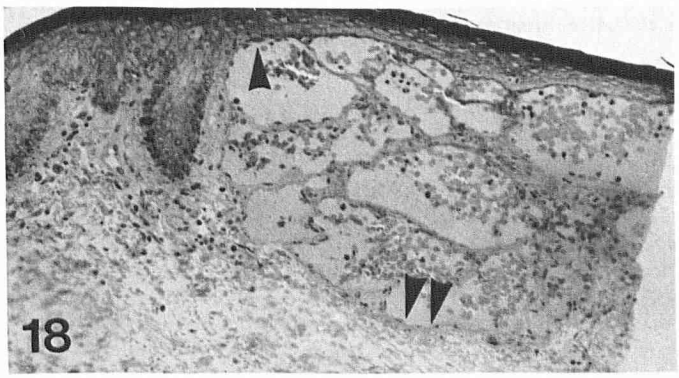

FIG 18. Histology of angiokeratoma (Fordyce). Portion of a single markedly widened dermal papilla containing a compact cluster of dilated vessels. Normal skin to left of vessels. Site indicated by *single arrowhead* had ultrastructure identical to that found at similar site shown in Fig 15. Site indicated by *2 arrowheads* had ultrastructure identical to that shown in Fig 17 except for absence of cellular inclusions. One-μm section, Spurr's resin, × 170.

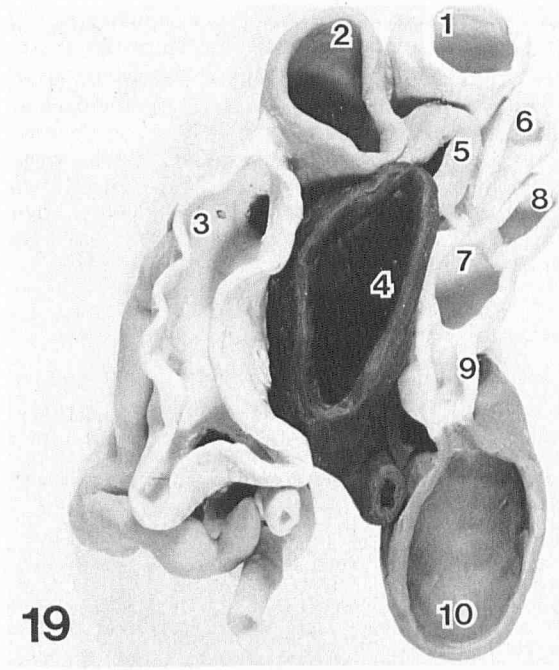

FIG 19. Clay model of angiokeratoma (Fordyce). Cross-section to show dilated saccules and their short narrow interconnections. *Numbers* correspond to those in Fig 20.

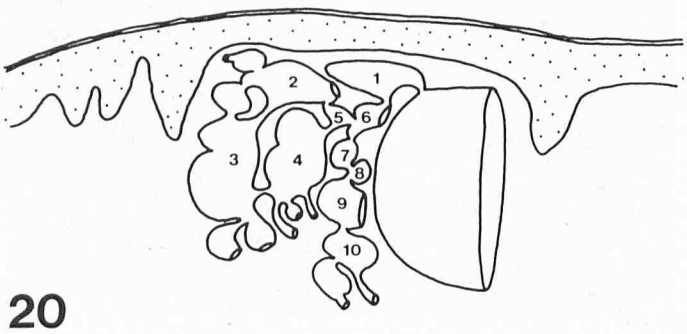

FIG 20. Schematic drawing of model of Fordyce angiokeratoma. Further sections after those used for constructing clay model in Fig 19 showed that the open saccules became closed and saccule *1* connected with a larger sac (not numbered). Two sets of connected saccules are present. One in a linear configuration *1-6-7-8-9-10* and one in ring formation *5-4-3-2-5* which connect at *5-6*. It is possible that *5-4-3-2* was originally linear but folded back on itself to form a ring. The entire cluster of vessels connected with a second cluster of vessels (not drawn) in the partially shown widened papilla to the right.

DISCUSSION

Mihm et al [5] and Higgins and Eady [6] have proposed, on the basis of observations made with light microscopic sections, that the upper horizontal plexus is a triple-layered network consisting of superficial and deep venular layers connected by shunts which enclose an intervening arteriolar layer. We did not find any evidence for such an organization. Rather we observed that arterioles and venules frequently coursed together in an undulatory manner through the papillary dermis. Some vessels from the superifical layers of the papillary dermis coursed toward the lower ones and some pursued sinuous paths between the upper and mid levels. When viewed in random sections by light microscopy, the undulating courses of such vessels could produce an illusion of a 3-tiered network.

The overall organization and ultrastructure of the dilated postcapillary venules in the 5 types of macular telangiectases appear to be identical. There could be quantitative differences in the proportion or density of venules that are affected to explain the variations in the clinical appearance of the macular telangiectases but we did not study these variables. All of the dilated postcapillary venules had thickened walls identical in appearance to those seen in the skin of patients with actinic damage [3], diabetes mellitus, various porphyrias [4], and chronologically aged skin [3]. Kint, Geerts, and Platevoet [7] made similar observations in their study of 2 cases of generalized essential telangiectasia, and we observed identical changes in the postcapillary venules composing cherry angiomas. It is unlikely that the etiology of the vascular wall thickening in these telangiectases is related to actinic damage because these vascular changes were also found in a lesion on the sun-protected, medial aspect of the upper arm and to a lesser degree in a telangiectatic mat on the tongue of a patient with scleroderma. Thickening of the vessel wall may prove to be a characteristic of macular and papular telangiectases originating from postcapillary venules.

Our findings indicate that the cherry angioma is a vascular lesion which appears to be derived from the venous limb of the capillary loop. Reconstruction of a portion of a pinpoint cherry angioma (0.2 mm) demonstrated a single tubular dilatation arising from the venous limb near the apex of a capillary loop. The larger cherry angiomas were composed of vessels having the ultrastructure of venous capillaries exhibiting endothelial bridged fenestrations and postcapillary venules, corroborating the findings of Stehbens and Ludatscher [8]. In our studies the majority of the vessels were venous capillaries. In addition, we found that the walls of the postcapillary venules were thickened by the peripheral deposition of a belt of basement membrane material admixed with reticulin fibers, an observation not mentioned by Stehbens and Ludatscher [8].

In the previous studies we had shown by autoradiography that the elongation of the capillary loops in the enlarging dermal papillae of psoriasis was associated with proliferation of endothelial cells both in the descending venous limb of the capillary loop and in the postcapillary venules of the horizontal plexus [9]. The following hypothesis is suggested for the pathogenesis of the cherry angioma. Factors, as yet undetermined, induce proliferation of endothelial cells in the venous limb of the capillary loop and in the postcapillary venules of the horizontal plexus so that the intrapapillary and extrapapillary portions of the capillary loop elongate. Subsequently or concomitantly with this elongation, focal dilatation in each loop is connected with its neighbor and the lesion grows by the centrifugal involvement of capillary loops in adjacent dermal papillae. The presence of postcapillary venules in the cherry angioma indicate that the descending extrapapillary portion of the loop also participates in its development and growth. When the vascular pattern in the 0.2-mm angioma is compared with that of the 1-mm lesion it seems clear that the growth of cherry angiomas proceeds in an organized and orderly fashion and that its growth does not represent neovascularization (proliferation of new vessels with randomly anastamosing channels).

The angiokeratomas of the scrotum (Fordyce) and of Fabry's disease did not resemble the cherry angioma in either ultrastructure or organization. The Fordyce and Fabry lesions exhibited an identical ultrastructure and were similar in their 3-dimensional organization even though the Fordyce lesion was larger and bulkier than the pinpoint Fabry lesion. In both angiokeratomas the dilated saccules were serially connected by very short narrow channels. The only apparent differences were the expected presence of the abnormal cellular inclusions and the unexpected finding of a deep dermal vascular connection in the angiokeratoma of Fabry's disease.

The ultrastructure of the vessels in the Fordyce and Fabry angiokeratomas is different from that of normal dermal microvessels. In the thinnest portions of the telangiectases, which were immediately adjacent to the epidermis, the endothelial cells rested on a moderately thickened, multilayered basement

membrane. In the thickest portions of the telangiectases, the vascular wall was composed of 2–4 layers of smooth muscle cells with intervening bundles of collagen fibers and rare elastic fibers. The basement membrane material in the wall had a homogeneous appearance. An internal elastic lamina was absent. The valve-containing dilated vessel in the deep dermis which was continuous with the superficial portion of the Fabry lesion had the same ultrastructure. We interpret the entire vascular entity in Fabry's disease to be a venule because of the multilayered basement membrane material in the vascular wall, the presence of valves, and the absence of an internal elastic lamina. Dermal arterioles with 2–4 layers of smooth muscle cells normally have a well-developed elastic lamina. Except for the presence of valves, the angiokeratomas of Fordyce and Fabry were identical in ultrastructure.

The ultrastructure of the Fabry and Fordyce lesions is identical to that of the small valve-containing collecting veins present at the interface of the dermis and subcutaneous fat which we have previously described [10]. In these small collecting veins which measure 70–120 μm in diameter, valves are situated at the branch points where the 30- to 50-μm dermal venules enter. The only difference between the vessels in the Fabry lesion and the normal small collecting veins is size (50 μm vs 70–120 μm in diameter, respectively). Our clinical observations confirm those of Bean who pointed out that the sites of Fordyce lesions tend to be superimposed on the course of the major collecting veins on the scrotum [11]. It is possible that the Fabry and Fordyce lesions represent the ectopic development or placement of small valve-containing collecting veins. Additional specimens of the Fabry and Fordyce angiokeratomas need to be studied in order to verify this hypothesis.

Ultrastructural studies of microvascular lesions have been limited primarily to the capillary or strawberry hemangiomas of infancy, which have been shown to be composed of venous capillaries and postcapillary venules [12–14], and the cavernous hemangiomas which exhibit the ultrastructural features consistent with small connecting veins [13]. The veil cells are numerous and well developed in capillary hemangiomas [14]. It is not known, however, whether these 2 common types of hemangiomas have a 3-dimensional organization analogous to that of the papular telangiectases, or whether they consist of new vessel formation with randomly anastamosing connections.

Two other telangiectases that have been studied are the spider angioma and the elevated puncta of hereditary hemorrhagic telangiectasia. A model of the former, constructed on the basis of serial paraffin-embedded sections, has been shown to be composed of an arteriole that connects to a presumed dilated venous saccule with radiating venous legs in the papillary dermis [15]. The elevated portion of the spider is thought to be produced by the venous elements. The lesions of hereditary hemorrhagic telangiectasia are thought to be venous on the basis of electron microscopy [16–18].

Our studies have shown that the macular and papular telangiectases are not produced by newly proliferating microvessels with random anastomoses, as might be concluded on the basis of routine paraffin sections. Rather, these telangiectases appear to have developed from alterations in the existing microvasculature with formation of recognizable 3-dimensional configurations in which specific segments of the microvasculature can be identified by electron microscopy.

We thank Dr. Gisela Moellmann for her helpful criticisms and suggestions in the preparation of this paper.

REFERENCES

1. Braverman IM, Yen A: Ultrastructure of the human dermal microcirculation: the horizontal plexus of the papillary dermis. J Invest Dermatol 66:131–142, 1976
2. McGrae JD, Winkelmann RK: Generalized essential telangiectasia. JAMA 185:909–913, 1963
3. Braverman IM, Fonferko E: Studies on cutaneous aging. II. The microvasculature. J Invest Dermatol 78:444–448, 1982
4. Epstein JH, Tuffanelli DL, Epstein WL: Cutaneous changes in the porphyrias. Arch Dermatol 107:689–698, 1973
5. Mihm MC Jr, Soter NA, Dvorak HF, Austen KF: The structure of normal skin and the morphology of atopic eczema. J Invest Dermatol 67:305–312, 1976
6. Higgins JC, Eady RAJ: Human dermal microvasculature: I. Its segmental differentiation. Light and electron microscopic study. Br J Dermatol 104:117–129, 1981
7. Kint A, Geerts M-L, Platevoet D: Generalized essential telangiectasia. Arch Belg Dermatol Syphiligr 28:377–385, 1972
8. Stehbens WE, Ludatscher RM: Fine structure of senile angiomas of human skin. Angiology 19:581–592, 1968
9. Braverman IM, Sibley J: Role of the microcirculation in the pathogenesis and treatment of psoriasis. J Invest Dermatol 78:2–17, 1982
10. Braverman IM, Keh-Yen A: Ultrastructure of the human dermal microcirculation IV. Valve-containing collecting veins at the dermal subcutaneous junction. J Invest Dermatol, 81:438–442, 1983
11. Bean WB: Vascular Spiders and Related Lesions of the Skin. Springfield, Ill, CC Thomas, 1958, p 265
12. Waldo ED, Vuletin JC, Kaye GI: The ultrastructure of vascular tumors: additional observations and a review of the literature. Pathol Annu 12:279–308, 1977
13. Iwanoto T, Jakobiec FA: Ultrastructural comparison of capillary and cavernous hemangiomas of the orbit. Arch Ophthalmol 97:1144–1153, 1979
14. Taxy JB, Gray SB: Cellular angiomas of infancy. An ultrastructural study of two cases. Cancer 43:2322–2331, 1979
15. Bean WB: Vascular Spiders and Related Lesions of the Skin. Springfield, Ill, CC Thomas, 1958, pp 45–50
16. Menefee MG, Flessa HC, Glueck H, Hoggs SP: Hereditary hemorrhagic telangiectasis (Osler-Weber-Rendu disease). Arch Otolaryngol 101:246–251, 1975
17. Hashimoto K, Pritzker MS: Hereditary hemorrhagic telangiectasia. An electron microscopic study. Oral Surg 34:751–768, 1972
18. Jahnke V: Ultrastructure of hereditary telangiectasia. Arch Otolaryngol 91:262–265, 1970